

Synthesis and Catalytic Activity of Iron Hydride Ligated with Bidentate N-Heterocyclic Silylenes for Hydroboration of Carbonyl Compounds

Xinghao Qi,[†] Tingting Zheng,^{†,‡} Junhao Zhou,^{†,‡} Yanhong Dong,[†] Xia Zuo,^{‡,§} Xiaoyan Li,^{*,†,§} Hongjian Sun,^{*,†,§} Olaf Fuhr,[§] and Dieter Fenske[§]

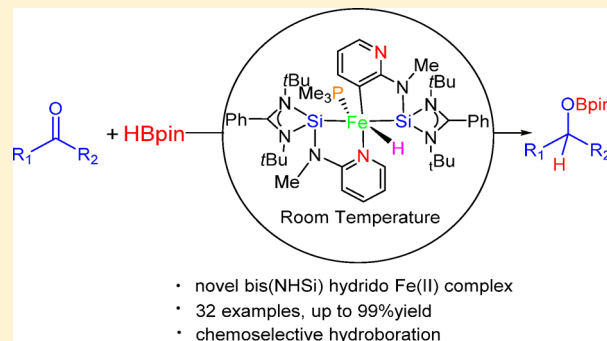
[†]School of Chemistry and Chemical Engineering, Key Laboratory of Special Functional Aggregated Materials, Ministry of Education, Shandong University, Shanda Nanlu 27, Jinan 250100, People's Republic of China

[‡]Department of Chemistry, Capital Normal University, Beijing 100037, People's Republic of China

[§]Institut für Nanotechnologie (INT) und Karlsruher Nano-Micro-Facility (KNMF), Karlsruher Institut für Technologie (KIT), Hermann-von-Helmholtz-Platz 1, 76344 Eggenstein-Leopoldshafen, Germany

Supporting Information

ABSTRACT: We report the synthesis of a novel bidentate N-heterocyclic silylene (NHSi) ligand, *N*-(LSi)-*N*-methyl-2-pyridinamine (**1**) (L = PhC(*Nt*Bu)₂), and the first bischelate disilylene iron hydride, [(Si,N)(Si,C)Fe(H)(PMe₃)] (**2**), and monosilylene iron hydride, [(Si,C)Fe(H)(PMe₃)₃] (**2'**), through C_{sp}²-H activation of the NHSi ligand. Compounds **1** and **2** were fully characterized by spectroscopic methods and single-crystal X-ray diffraction analysis. Density functional theory calculations indicated the multiple-bond character of the Fe–Si bonds and the π back-donation from Fe(II) to the Si(II) center. Moreover, the strong donor character of ligand **1** enables **2** to act as an efficient catalyst for the hydroboration reaction of carbonyl compounds at room temperature. Chemoselective hydroboration is attained under these conditions. This might be the first example of hydroboration of ketones and aldehydes catalyzed by a silylene hydrido iron complex. A catalytic mechanism was suggested and partially experimentally verified.



INTRODUCTION

In recent years, the design of novel N-heterocyclic silylenes (NHSis) and the construction of NHSi-ligated metal complexes have received increasing interest.¹ Compared with N-heterocyclic carbenes (NHCs), the divalent Si center in a singlet state has unique σ -donating/ π -accepting and steric hindrance properties. Therefore, transition metal complexes with NHSi ligands have been proved to be highly active precatalysts in the Suzuki² and Heck³ coupling reactions, reduction of amides,⁴ borylation⁵ and amination of arenes,⁶ the [2 + 2 + 2] cyclotrimerization reaction of phenylacetylene,⁷ hydrosilylation of alkenes⁸ or ketones,⁹ and Sonogashira¹⁰ and Kumada¹¹ cross-coupling reactions. However, there are few reports on multidentate NHSi ligands, and NHSi-ligated hydrido metal complexes remain virtually unknown.

Hydroboration of carbonyl compounds has found widespread application in conversion into the corresponding alcohols.¹² However, most of the studies on these reactions have focused on transition metals (Ru,¹³ Cu,¹⁴ Ti,¹⁵ Mo,¹⁶ Mn,¹⁷ and Zn¹⁸), main-group elements (Li,¹⁹ Mg,²⁰ Ca,²¹ Al,²² Ga,²³ Ge,²⁴ Sn,²⁴ and P²⁵), and lanthanides²⁶ as catalysts. Only a few cases have been reported to be catalyzed by base metals.²⁷ Tamang and Findlater²⁸ utilized Fe(acac)₃ to achieve efficient conversion for

the hydroboration of aldehydes and ketones. More recently, Baker and co-workers reported the remarkable catalytic activity of an imine-coupled [Fe–N₂S₂]₂ complex in the selective hydroboration of various aliphatic and aromatic aldehydes. Although hydrido iron complexes are postulated as key intermediates in these catalytic mechanisms,²⁹ there is no report on efficiently catalyzed hydroboration of carbonyl compounds by hydrido iron complexes.

A variety of hydrido metal complexes are now employed in catalytic synthetic chemistry, coordination chemistry, and homogeneous catalysis. Recently, our group obtained the first example of cobalt(III) hydride supported by chlorosilylene.³⁰ This complex displayed a more efficient catalytic ability for the Kumada cross-coupling reaction than the hydrido Co(III) chloride stabilized by the trimethylphosphine ligand. Inspired by these results, in this work we synthesized *N*-(LSi)-*N*-methyl-2-pyridinamine (**1**) (L = PhC(*Nt*Bu)₂) as a new example of a bidentate silylene ligand and the hydrido iron(II) complex [(Si,N)(Si,C)Fe(H)(PMe₃)] (**2**) in an unexpected coordination mode. Complex **2** can act as an efficient precatalyst for

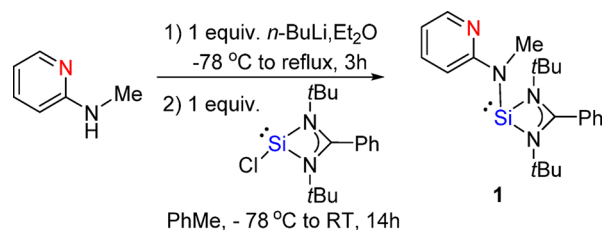
Received: September 26, 2018

hydroboration reactions of various ketones and aldehydes at room temperature with low catalyst loading.

RESULTS AND DISCUSSION

Synthesis of the Bidentate N-Heterocyclic Silylene Ligand. Given the interest in approaches for the synthesis of base stabilized NHSis,^{5a,6,7,9b} we intended to synthesize the pyridine-based bidentate ligand via a salt metathesis reaction of *N*-methyl-2-pyridinamine as the backbone (Scheme 1). After

Scheme 1. Synthesis of the Bidentate NHSi Ligand 1



lithiation of the precursor with 1 equiv of *n*-BuLi in diethyl ether, a toluene solution of 1 equiv of the chlorosilylene LSi:Cl was added dropwise to the reaction mixture at $-78\text{ }^{\circ}\text{C}$ to afford the desired bidentate NHSi compound **1** in 88% yield. In the ^1H NMR spectrum of **1**, two singlets for the *t*Bu and Me groups appear at 1.05 and 3.26 ppm, respectively, with an integral ratio of 18:3. One signal of Si(II) exists at 12.0 ppm in the ^{29}Si NMR spectrum of **1**. This chemical shift is comparable to the value of 14.6 ppm for chlorosilylene reported by Roesky and co-workers.³¹

The molecular structure of compound **1** is shown in Figure 1. In the solid state, the silicon atom is three-coordinate ($3 \times \text{N}$)

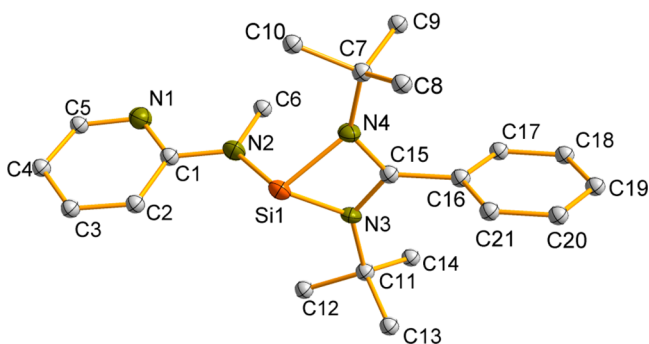
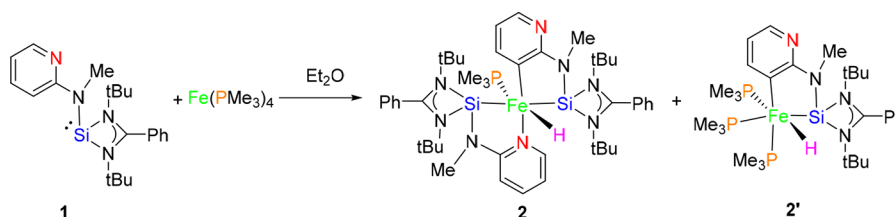


Figure 1. Molecular structure of ligand **1**. The ORTEP representation of **1** is shown at the 50% probability level (H atoms have been omitted for clarity). Selected bond lengths (\AA) and angles ($^{\circ}$): Si1–N2 1.782(2), Si1–N3 1.885(2), Si1–N4 1.875(2), N2–C1 1.384(3); N3–Si1–N2 102.11(8), N4–Si1–N2 102.81(8), N4–Si1–N3 69.10(7), C1–N2–Si1 122.00(2).

Scheme 2. Synthesis of Bis(NHSi) Hydrido Fe(II) Complex 2



B

and features a trigonal-pyramidal geometry. The angle of 112.0° between the Si1–C15–N3–N4 plane and the Si1–N2 bond illustrates the predominant character of the silicon center with a lone pair. Si1–N3 (1.885(2) \AA) and Si1–N4 (1.875(2) \AA) are longer than Si1–N2 (1.782(2) \AA). It is obvious that the lone pair of electrons on the Si atom occupies the vertex of the trigonal pyramid, emphasizing the predominant silylene character. The sum of the four inner angles of the Si1–N3–C15–N4 ring is 356.7° , deviating from 360° . This shows that the four atoms are not completely coplanar. The phenyl ring is almost parallel to the pyridine ring and perpendicular to the four-membered cycle.

Reaction of $\text{Fe}(\text{PMe}_3)_4$ with Bidentate N-Heterocyclic Silylene Ligand 1. Compound **1** is a potential chelating ligand because of the good coordination abilities of the nitrogen atom on the pyridine ring and the silylene Si atom. Surprisingly, the reaction of bidentate preligand **1** with $\text{Fe}(\text{PMe}_3)_4$ in diethyl ether resulted in the formation of air-sensitive bis(NHSi) hydrido Fe(II) complex **2** with an unexpected coordination mode (Scheme 2). On the one hand, one molecule of **1** is (Si,N)-chelate-coordinated to the Fe center; on the other hand, the other molecule of **1** is (Si,C)-chelate-coordinated to the Fe atom via $\text{C}_{\text{sp}^2}\text{--H}$ bond activation of the pyridine ring. Complex **2** was isolated as dark-red crystals from *n*-pentane at $0\text{ }^{\circ}\text{C}$ in 85% yield. To the best of our knowledge, **2** is the first example of a silylene hydrido iron(II) complex produced through activation of the $\text{C}_{\text{sp}^2}\text{--H}$ bond of the pyridine ring in the NHSi ligand.

In the infrared spectrum of complex **2**, the typical stretching band for the Fe–H bond was found at 1900 cm^{-1} . The ^1H NMR spectrum of **2** in C_6D_6 provides evidence for the hydrido ligand at -10.68 ppm as a doublet due to coupling of the hydrido H with the coordinated P atom ($^2J_{\text{P,H}} = 9\text{ Hz}$). The signal of the PMe_3 ligand appears at 15.7 ppm as a singlet in the ^{31}P NMR spectrum of **2**. In the ^{29}Si NMR spectrum of **2**, the signals of two kinds of Si(II) atoms were detected at 48.7 and 59.6 ppm as two doublets with $^2J_{\text{Si,P}}$ coupling constants of 29.8 and 23.8 Hz, respectively, showing the inequivalence of the two silylene moieties.

Single-crystal X-ray diffraction data for complex **2** confirmed a distorted hexacoordinate octahedral geometry around the Fe(II) center (Figure 2). The axial H126–Fe1–P4 moiety ($175(1)^{\circ}$) is almost perpendicular to the equatorial plane formed by Fe1, Si2, N6, Si3, and C15. The sum of the coordination bond angles in the equatorial plane is 351.87° , which deviates significantly from 360° . This result illustrates that the five atoms are not within one plane. The Fe1–H126 bond length of 1.48(3) \AA is within the normal scope of Fe–H bond lengths.³² A summary of the Fe–Si bond distances for silylene \rightarrow Fe complexes is presented in Table 1. The Fe–Si bond distances in complex **2** are shorter than those in the silylene \rightarrow Fe(CO)₄ and silylene \rightarrow Fe(dmpe)₂ complexes. Moreover, they are comparable to the silylene \rightarrow Fe bond distances with formal

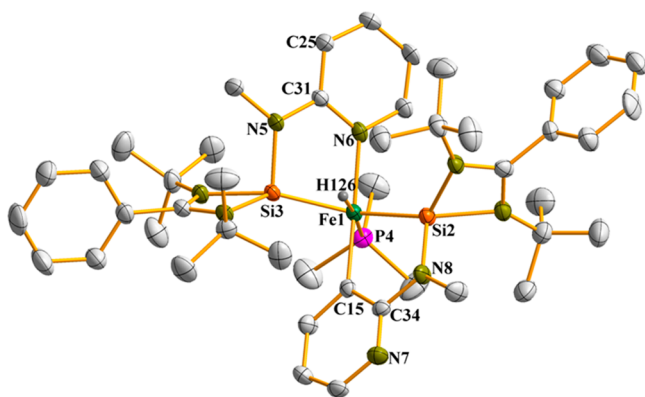


Figure 2. Molecular structure of complex **2**. The ORTEP representation of complex **2** is shown at the 50% probability level (most of the H atoms have been omitted for clarity). Selected bond lengths (Å) and angles (deg): Fe1–Si2 2.177(1), Fe1–Si3 2.159(1), Fe1–P4 2.190(1), Fe1–N6 2.045(3), Fe1–C15 2.010(3), Fe1–H126 1.48(3); C15–Fe1–Si2 81.5(1), C15–Fe1–Si3 94.2(1), N6–Fe1–Si2 93.76(8), N6–Fe1–Si3 82.38(8), H126–Fe1–P4 175(1).

Table 1. Comparison of the Fe–Si Distances in Silylene→Fe Complexes

compound	Fe–Si (Å)	ref
[<i>:Si</i> (<i>Nt</i> BuCH ₂) ₂] <i>Fe</i> (CO) ₄	2.196	33
[<i>:Si</i> (<i>Ot</i> Bu){(<i>Nt</i> Bu) ₂ CPh}] <i>Fe</i> (CO) ₄	2.237(7)	34
[<i>:Si</i> (NHC)(H) <i>Si</i> (<i>t</i> Bu) ₃] <i>Fe</i> (CO) ₄	2.3717(16)	35
[<i>:Si</i> (X){(<i>Nt</i> Bu) ₂ CPh}] <i>Fe</i> (<i>dmpe</i>) ₂	2.1634(9) (X = Cl)	9a
	2.200(2) (X = Me)	9a
	2.184(2) (X = H)	9a
Cp* <i>Fe</i> (CO)(<i>SiMe</i> ₃) <i>SiMes</i> ₂	2.154(1)	36
[<i>Si</i> (N <i>Si</i>) <i>Fe</i> (PMe ₃) ₂	2.1579(15), 2.1664(15)	9b
complex 2	2.159(1), 2.177(1)	this work

double bonds between Fe and Si, indicating the multiple-bond character. The Fe1–Si3 bond distance (2.159(1) Å) is shorter than the Fe1–Si2 bond distance (2.177(1) Å), potentially indicating stronger π -acceptor character of Si3 versus Si2. This is reasonable because the coordination of the nitrogen atom on the pyridine ring causes electron deficiency at Si3. This is consistent with the comparison of the natural bond orbital (NBO) charges of C31 and C34 (Table 2).

To our surprise, from the mother solution for the reaction of *Fe*(PMe₃)₄ with ligand **1**, a small amount of monosilylene hydrido iron complex **2'** as a byproduct was obtained as a red

Table 2. NBO Charges, Wiberg Bond Indices (WBIs), and Selected Calculated Bond Lengths for Complex **2**^a

atom	NBO charge	bond	WBI	bond length (Å)
Fe1	−0.356	Fe1–Si2	1.0978	2.240
Si2	+1.423	Fe1–Si3	1.1705	2.187
Si3	+1.394	Fe1–P4	0.9357	2.278
P4	+1.065	Fe1–N6	0.5521	2.107
N6	−0.470	Fe1–C15	0.8138	2.044
C15	−0.251	Fe1–H126	0.6109	1.537
H126	−0.105			
C31	0.44082			
C34	0.38221			

^aLevel of theory: B3LYP functional with the 6-31G(d,p) basis set for C, H, N, P, and Si and the LANL2DZ basis set for Fe.

powder. In the infrared spectrum of **2'**, the typical stretching band for the Fe–H bond was found at 1920 cm^{−1}. Compared with that of complex **2** (1900 cm^{−1}), this is a hypsochromic shift due to the fact that there is only one π back-donation from Fe to Si. The hydrido H signal in the ¹H NMR spectrum of **2'** is located at −15.66 ppm as a doublet of doublets of doublets caused by the multiple P–H couplings (²J_{P,H} = 9 Hz, ²J_{P,H} = 21 Hz, ²J_{P,H} = 51 Hz). In the ³¹P NMR spectrum of **2'**, the signals of three PMe₃ ligands appear at 37.9 (t, ²J_{P,P} = 36 Hz), 30.9 (dd, ²J_{P,P} = 48 Hz, 24 Hz), and 28.5 (m) respectively, indicating that the three PMe₃ ligands in **2'** have different chemical environments, as shown in Scheme 2. In the ²⁹Si NMR spectrum of **2'**, a signal at 57.8 ppm caused by the P–Si couplings (ddd, ²J_{P,Si} = 89.1 Hz, 49.5 Hz, 19.8 Hz) is comparable with the values of 48.7 and 59.6 ppm for complex **2**. It must be noted that an efficient synthesis of **2'** has not been realized by adjusting the reactant ratio and reaction temperature. It is probable that **2'** is an intermediate in the formation of **2**.

We deduce that the reaction in Scheme 2 begins with the ligand replacement of PMe₃ by NHSi **1** to afford intermediate **A1** (Scheme 3). This precoordination brings the iron close to the C–H bond of **1** and results in the cleavage of the C–H bond to form intermediate **2'** as an iron(II) hydride. Complex **2'** is not stable and can be further transformed to **2** by the second ligand replacement of two PMe₃ ligands by **1** with the chelate effect. Complex **2** is thermodynamically stabilized by one neutral (Si,N)-chelate ligand and one anionic (Si,C)-chelate ligand.

To further clarify the electronic structure of the iron center in **2**, we particularly performed detailed density functional theory (DFT) calculations at the B3LYP/6-31G(d,p)/LANL2DZ[Fe] level of theory.³⁷ Reasonable agreement exists between the bond lengths with the Fe center found in the geometry-optimized structures and those observed by X-ray structure determinations. The lengths of the two Fe–Si bonds are 2.240 and 2.187 Å, respectively, which are slightly longer than the experimentally determined values in **2**. The pertinent calculated structural parameters of **2** are presented in Table 2.

The calculated NBO charges on the donor atoms indicate the heavy polarization of the bonds with the Fe center. The NBO charges on the Si atoms are slightly less positive and point to enhanced π back-donation from the Fe(II) center to Si(II). Furthermore, the calculated Wiberg bond indices (WBIs) for complex **2** differ for each donor atom with the Fe center. The values for the Fe–Si bonds (WBI > 1) clearly indicate some multiple-bond character.³⁸

Figure 3 shows the energies and shapes of the frontier molecular orbitals of complex **2**. The HOMO and HOMO−1 also show the multiple-bond character of the Fe–Si bond through π back-donation from the distorted d_{x²−y²} and d_{yz} orbitals of the Fe center to the 3p orbitals of the Si(II) atom. It is important to note that the polarization of the frontier molecular orbitals shows the inequivalence of the two NHSi ligands. Moreover, the LUMO in complex **2** is centered on the phenyl ring of one NHSi ligand.

Catalytic Activity of Complex 2 for Hydroboration of Carbonyl Compounds. Currently, iron catalysts are being applied more and more in various organic synthetic reactions. Hydrido iron complexes often play an important role in the catalytic cycle. Some hydrido iron complexes have been used to establish efficient catalytic systems for hydrogenation³⁹ and hydrosilylation processes.⁴⁰ Encouraged by these results, we were interested in exploring the catalytic ability of complex **2** for the hydroboration of carbonyl compounds.

Scheme 3. Pathway from Ligand 1 to Complex 2

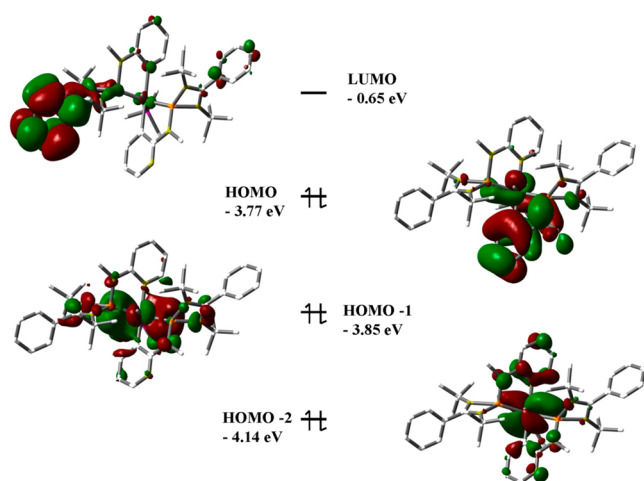
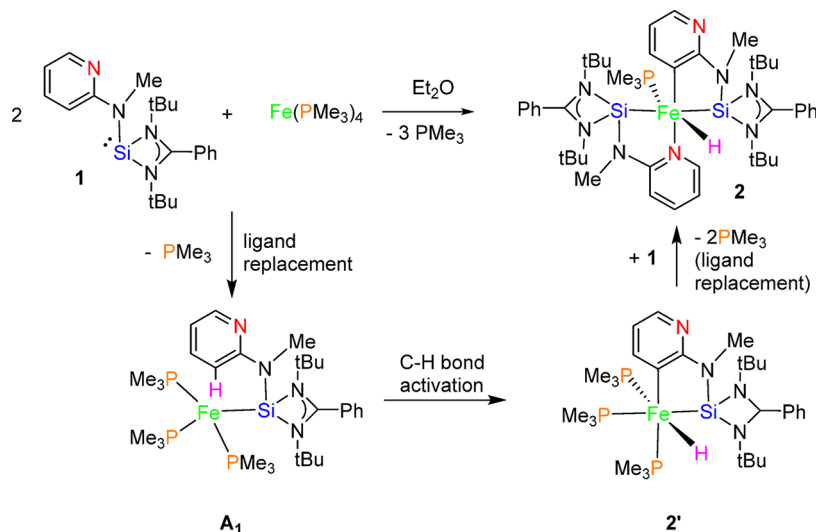


Figure 3. Selected molecular orbitals of complex 2 calculated at the B3LYP/6-31G(d,p)/LANL2DZ[Fe] level of theory.

The studies of the influence of the reaction conditions were carried out with acetophenone as a model substrate using pinacolborane in THF at room temperature (Table 3). The control experiment without catalyst confirmed that hydroboration of acetophenone is a catalytic process. When the reaction mixture was stirred at room temperature for 6 h, no reaction was observed (Table 3, entry 1). However, when iron(II) hydride 2 was added as a catalyst, conversion of acetophenone was realized. To our delight, 99% conversion was observed in the presence of 1 mol % 2 (Table 3, entry 5). When the reaction temperature was raised to 50 °C, the substrate was completely transformed after 2 h. However, we decided to focus on exploring convenient catalytic conditions for operation and chose to explore further conditions at room temperature. The conversion decreased significantly with a decrease in the catalyst loading (Table 3, entry 2) or with shortening of the reaction time (Table 3, entries 3–5). It was found that THF was the best reaction medium in comparison with the other tested solvents (Table 3, entries 6–10).

Under the optimized experimental conditions, we examined the scope of the hydroboration with a variety of ketones (Table 4). The purification of hydroborated products by SiO₂ column

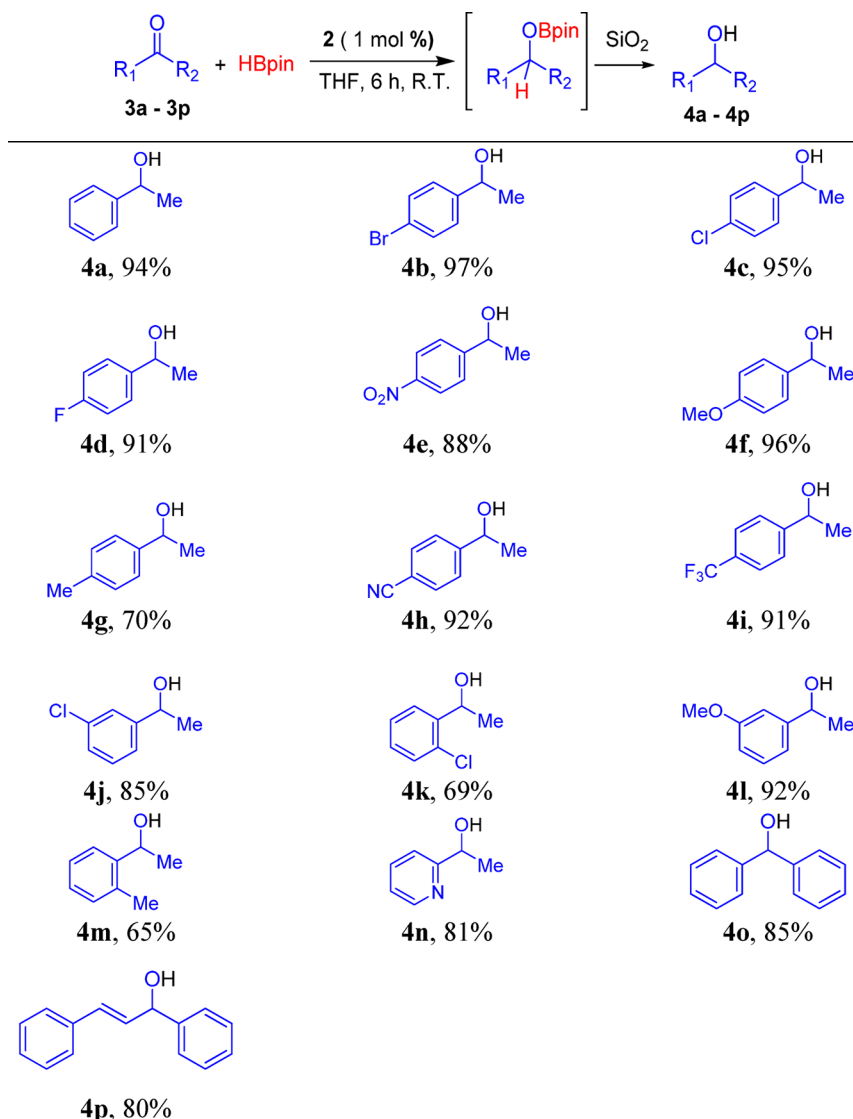
Table 3. Catalytic Results for the Probe Reaction between Acetophenone and Pinacolborane^a

entry	loading (mol %)	solvent	time (h)	conv. (%) ^b
1	0	THF	6	0
2	0.5	THF	6	90
3	1	THF	2	67
4	1	THF	4	92
5	1	THF	6	99
6	1	Et ₂ O	6	66
7	1	DMSO	6	32
8	1	dioxane	6	48
9	1	toluene	6	51
10	1	DMF	6	17

^aCatalytic conditions: PhCOCH₃ (1.0 mmol) and HBpin (1.1 mmol) in 2 mL of solvent. ^bDetermined by GC with *n*-dodecane as an internal standard.

chromatography led uniquely to the isolation of 2° alcohols 4 via silica-promoted hydrolysis of alkoxyboronate pinacol esters. A high isolated yield of 1-phenylethanol (4a) was achieved. Acetophenones with electron-withdrawing substituents at the para position were hydroborated effectively, affording the corresponding alcohols in good to excellent yields (4a–d). This iron-catalyzed hydroboration reaction of ketones tolerates various functionalities, including nitro (4e), ether (4f, 4l), cyano (4h), trifluoromethyl (4i), and alkenyl (4p) moieties. Moderate yields were obtained for acetophenones with strong electron-donating Me groups at the ortho or para position (4g, 4m). 1-(2-pyridyl)ethanol (4n) was isolated in a yield of 81%. As expected, steric hindrance factors also led to a reduction in the isolated yield (4j, 4k, 4o). An α,β -unsaturated ketone was selectively reduced to the α,β -unsaturated alcohol (4p).

Furthermore, the catalytic reactions of derivatives of benzaldehyde took place for a shorter time in excellent yields because they are more active than ketones (Table 5). Benzyl alcohol (6a) was isolated in quantitative yield. Notably, high yields of the corresponding alcohols (6b–f, 6i) were achieved in

Table 4. Scope of Hydroboration of Ketones^{a,b}

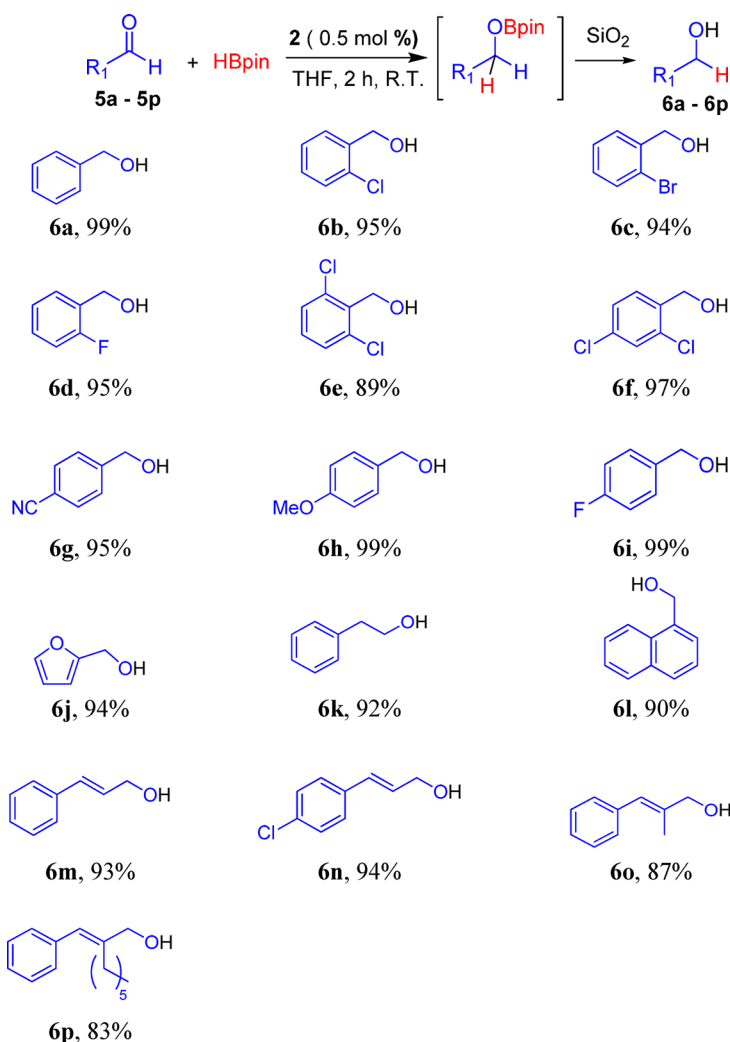
^aCatalytic conditions: substrate (1.0 mmol) and HBpin (1.1 mmol) in 2 mL of THF at rt. ^bIsolated yields are shown.

the presence of halide substituents irrespective of their positions on the phenyl ring. The benzaldehydes with CN and MeO groups at the para position provided quantitative conversion (**6g**, **6h**). When phenylacetaldehyde was subjected to the catalysis, 1-phenylethyl alcohol (**6k**) was isolated in 92% yield. For other aromatic aldehydes, such as furan-2-carbaldehyde and 1-naphthaldehyde, excellent yields were obtained for this catalytic system (**6j**, **6l**). Interestingly, **2** exhibited excellent selectivity for the hydroboration of the C=O bond of α,β -unsaturated aldehydes in excellent yields (**6m-p**).

The chemoselective hydroboration of different carbonyl substrates was studied (Scheme 4). These results are consistent with previous reports.^{19b,21,26c,d,28} It is obvious that the chemoselectivity is determined by the two molecular moieties linked with carbonyls. The competitive intermolecular catalytic hydroboration of benzaldehyde and acetophenone resulted in almost exclusive conversion of the aldehyde (Scheme 4a). The competitive hydroboration between *p*-fluorobenzaldehyde and *p*-methoxybenzaldehyde gave rise to *p*-fluorobenzyl borate as the main product (Scheme 4b), and the similar reaction with *p*-fluoroacetophenone and *p*-methylacetophenone delivered the

related *p*-fluorobenzyl borate as the main product (Scheme 4c). Similar chemoselectivities for benzaldehyde and cinnamaldehyde were observed in the competitive reactions of benzaldehyde, cinnamaldehyde, and acetophenone (Scheme 4d). Until the addition of 2.2 equiv of HBpin, only the equivalent conversions of the aldehydes were achieved. This also shows that the conjugated C=C double bond of the α,β -unsaturated aldehyde has no effect on the selectivity. These results indicate that this catalytic system allows the chemoselective conversion of aldehydes to the related borates even in the presence of ketones. From Scheme 4 we know that the substrates (aldehydes or ketones) with electron-withdrawing groups are preferentially reduced.

Study of the Catalytic Reaction Mechanism. To understand the intermediates involved in this efficient hydroboration, the following two experiments were designed (Scheme 5). It was verified that no reaction between complex **2** and HBpin occurred at room temperature in the first experiment. In contrast, the brown solution of **2** changed quickly to dark red upon addition of *p*-fluorobenzaldehyde, showing that reaction had taken place. Our attempts to isolate **2c** proved to be

Table 5. Scope of Hydroboration of Aldehydes^{a,b}

13

^aCatalytic conditions: substrate (1.0 mmol) and HBpin (1.1 mmol) in 2 mL of THF at rt for 2 h. ^bIsolated yields are shown.

unsuccessful. It is likely that **2c** is very unstable. However, the disappearance of signals for $\nu(\text{H}-\text{Fe})$ and $\rho(\text{PCH}_3)$ was obviously observed in the infrared spectrum, indicating breaking of the H–Fe bond and dissociation of PMe_3 . Concomitantly, the signal of H–Fe (–10.68 ppm) disappeared in the in situ ^1H NMR spectrum. These results imply that the catalytic cycle for iron hydride-catalyzed hydroboration of aldehydes and ketones involves the insertion of the carbonyl group into an Fe–H bond, giving the possible reactive intermediate **2c**, which was further detected by MS.

On the basis of the above results and the precedent of metal-catalyzed hydroboration reactions of carbonyl compounds,^{14,24,28} we propose a possible catalytic cycle for this hydrido iron complex-catalyzed hydroboration reaction (Scheme 6). At first, the dissociation of PMe_3 group takes place to form highly active iron hydride intermediate **2a** as the real catalyst with a vacant coordination site. Subsequently, coordination of the oxygen atom of the carbonyl group to the metal center enhances the polarity of the C=O bond, making it easier to insert the Fe–H bond and generate intermediate **2c**. In the presence of HBpin, **2c** delivers the alkoxyboronate pinacol

ester via B–H bond activation with recovery of the real catalyst **2a**.

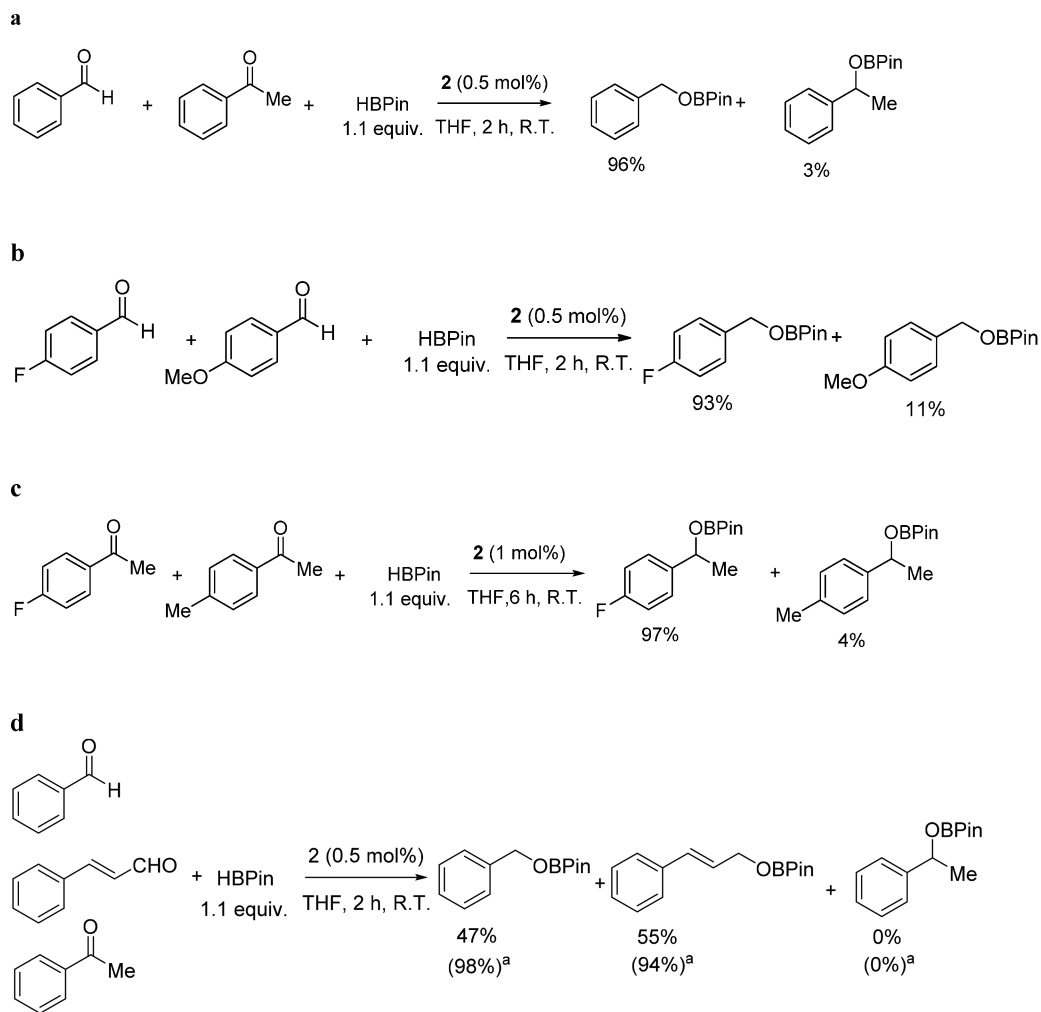
CONCLUSION

The novel N-heterocyclic silylene **1** was synthesized by the salt metathesis reaction of *N*-methyl-2-pyridinamine with a chlorosilylene. We also successfully obtained the first bis-(NHSi)-chelated hydrido Fe(II) complex **2** and mono(NHSi)-chelated hydrido Fe(II) complex **2'** via chelate-assisted $\text{C}_{\text{sp}^2}\text{-H}$ bond activation of **1**. Similarly, the hydroboration reactions of carbonyl compounds were proved for the first time to be efficiently catalyzed by the iron hydride at room temperature. A novel iron hydride-catalyzed mechanism was suggested and was partially experimentally verified.

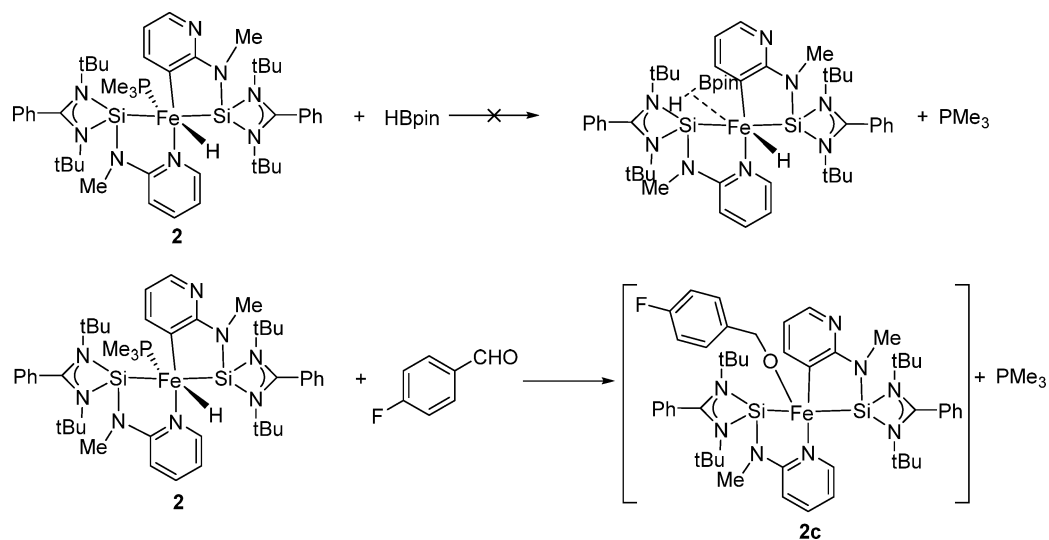
EXPERIMENTAL SECTION

General Procedures and Materials. All air-sensitive and volatile materials were processed under a nitrogen atmosphere using standard vacuum techniques. Diethyl ether, *n*-pentane, THF, and toluene were dried and distilled under nitrogen according to known methods before use. $\text{Fe}(\text{PMe}_3)_4$ ⁴¹ and the chlorosilylene⁴² were prepared according to the known literature methods. All of the other chemicals were purchased and used as received without further purification. Infrared

Scheme 4. Chemoselective Hydroboration Reactions



Scheme 5. Investigation of the Mechanism

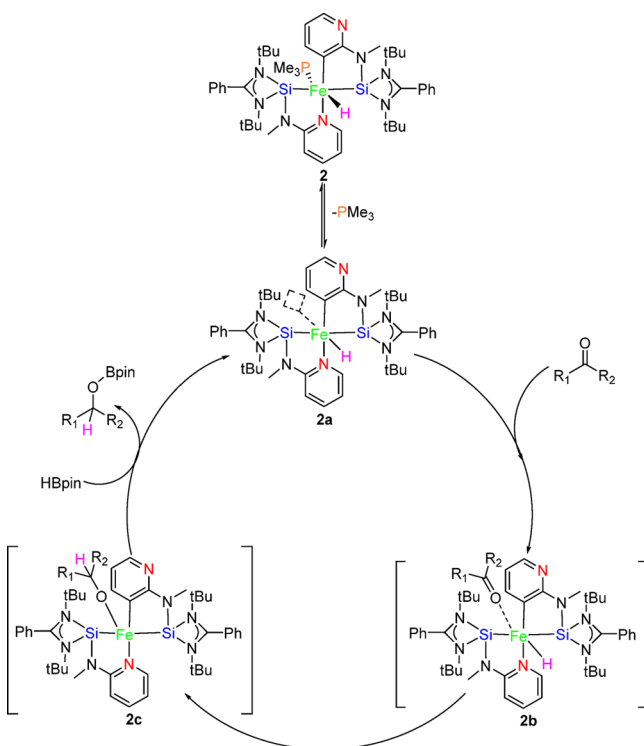


spectra (4000–400 cm^{-1}) were obtained from Nujol mulls between KBr disks and recorded on a Bruker ALPHA FT-IR instrument. ^1H , $^{13}\text{C}\{^1\text{H}\}$, $^{31}\text{P}\{^1\text{H}\}$, and $^{29}\text{Si}\{^1\text{H}\}$ NMR spectra were recorded on Bruker Avance 300 and 600 MHz spectrometers. Gas chromatography was

performed with *n*-dodecane as an internal standard. Elemental analyses were carried out on an Elementar Vario ELIII instrument.

Synthesis of *N*-Methyl-2-pyridinamine.⁴³ Under a N_2 atmosphere, copper powder (0.1 g, 1.6 mmol), 2-bromopyridine (5.4 g, 34.2 mmol), and 30 mL of methylamine solution in water (25%) were added

Scheme 6. Proposed Mechanism for Iron-Catalyzed Hydroboration of Carbonyl Compounds



to a 100 mL Schlenk tube containing a magnetic stirrer. The reaction mixture was stirred at 95 °C for 48 h. After cooling, the product was extracted with 150 mL of ethyl acetate three times and dried over Na₂SO₄. After filtration, volatile materials were evaporated in vacuo. The crude product was purified by column chromatography over silica gel with a mixture of petroleum ether and ethyl acetate (1:2) as an eluent. The product was further purified by vacuum distillation in a yield of 56%.

Synthesis of Compound 1. A 3.63 mL sample of *n*-BuLi (2.5 M in hexane, 9.1 mmol) was added slowly to 40 mL of a diethyl ether solution of *N*-methyl-2-pyridinamine (0.98 g, 9.1 mmol) at −78 °C, forming a yellowish suspension, which was warmed to room temperature and then refluxed for 3 h. The resulting solution was cooled to −78 °C, and a solution of the chlorosilylene (2.67 g, 9.1 mmol) in 30 mL of toluene was added dropwise via funnel. The color changed to orange with the addition. All of the volatiles were removed in vacuum after overnight stirring. The product was extracted with 80 mL of *n*-pentane, and the residual precipitate was removed by filtration. The solution was concentrated to 60 mL and placed at 0 °C over 2 days, affording colorless crystals. Yield: 2.93 g (88%). Dec. >168 °C. Anal. Calcd for C₂₁H₃₀N₄Si (366.22 g mol^{−1}): C, 68.81; H, 8.25; N, 15.28. Found: C, 69.19; H, 8.00; N, 15.47. IR (Nujol mull, KBr, cm^{−1}): 1594 ν(C=N), 1552 ν(C=C). ¹H NMR (300 MHz, C₆D₆, 298 K, ppm): 1.05 (s, 18H, C(CH₃)₃), 3.26 (s, 3H, CH₃), 6.47–8.51 (m, 9H, Ar-H). ¹³C NMR (150 MHz, C₆D₆, 298 K, ppm): 30.9 (C(CH₃)₃), 52.5 (C(CH₃)₃), 111.2 (C_{arom}), 113.0 (C_{arom}), 127.3 (C_{arom}), 127.9 (C_{arom}), 128.0 (C_{arom}), 129.1 (C_{arom}), 129.7 (C_{arom}), 133.8 (C_{arom}), 135.1 (C_{arom}), 148.1 (NCN). ²⁹Si NMR (59.59 MHz, C₆D₆, 298 K, ppm): −12.0 (s).

Synthesis of Complexes 2 and 2′. A solution of ligand **1** (1.0 g, 2.73 mmol) in diethyl ether (30 mL) was added slowly to a solution of Fe(PMe₃)₄ (0.49 g, 1.37 mmol) in diethyl ether (30 mL) at −78 °C. The reaction mixture was allowed to stir for 14 h at room temperature. The solvents were removed under vacuum, and the residue was extracted with 60 mL of *n*-pentane. Dark-red crystals of **2** were obtained at 0 °C. Yield: 1.00 g (85%). Mp: 137–138 °C. Anal. Calcd for C₄₅H₆₉FeN₈PSi₂ (865.09 g mol^{−1}): C, 62.48; H, 8.04; N, 12.95. Found: C, 62.82; H, 8.17; N, 13.16. IR (Nujol mull, KBr, cm^{−1}): 3056 ν(H–

C=C), 1900 ν(H–Fe), 937 ρ(PCH₃). ¹H NMR (300 MHz, C₆D₆, 298 K, ppm): −10.68 (d, ²J_{P,H} = 9 Hz, 1H, Fe–H), 0.97 (s, 18H, C(CH₃)₃), 1.02 (s, 18H, C(CH₃)₃), 1.78 (d, 9H, ²J_{P,H} = 6 Hz, PCH₃), 2.92 (s, 3H, CH₃), 3.56 (s, 3H, CH₃), 6.16–9.54 (m, 17H, Ar–H). ³¹P NMR (121 MHz, C₆D₆, 298 K, ppm): 15.7 (s, P(CH₃)₃). ¹³C NMR (75 MHz, C₆D₆, 298 K, ppm): 28.9 (P(CH₃)₃), 29.8 (CH₃), 31.4 (C(CH₃)₃), 31.7 (C(CH₃)₃), 32.0 (C(CH₃)₃), 32.7 (CH₃), 53.0 (C(CH₃)₃), 54.0 (C(CH₃)₃), 54.6 (C(CH₃)₃), 104.1 (C_{arom}), 108.5 (C_{arom}), 110.5 (C_{arom}), 126.9 (C_{arom}), 128.9 (C_{arom}), 129.2 (C_{arom}), 129.4 (C_{arom}), 129.6 (C_{arom}), 130.5 (C_{arom}), 130.6 (C_{arom}), 133.8 (C_{arom}), 134.6 (C_{arom}), 137.7 (C_{arom}), 140.7 (C_{arom}), 152.7 (C_{arom}), 154.8 (C_{arom}), 162.1 (C_{arom}), 167.0 (C_{arom}), 169.5 (NCN), 173.4 (NCN). ²⁹Si NMR (59.59 MHz, C₆D₆, 298 K, ppm): 48.7 (d, ²J_{P,Si} = 29.8 Hz), 59.6 (d, ²J_{P,Si} = 23.8 Hz).

Complex **2′** was obtained as a red powder in very low yield. IR (Nujol mull, KBr, cm^{−1}): 1920 ν(H–Fe), 922 ρ(PCH₃). ¹H NMR (300 MHz, C₆D₆, 298 K, ppm): −15.66 (ddd, ²J_{P,H} = 9 Hz, 21 Hz, 51 Hz, 1H, Fe–H), 1.06 (s, 9H, PCH₃), 1.18 (s, 18H, C(CH₃)₃), 1.29 (d, 9H, ²J_{P,H} = 3 Hz, PCH₃), 1.46 (d, 9H, ²J_{P,H} = 3 Hz, PCH₃), 3.39 (s, 3H, CH₃), 6.63–8.39 (m, 8H, Ar–H). ³¹P NMR (121 MHz, C₆D₆, 298 K, ppm): 37.9 (t, ²J_{P,P} = 36 Hz, 1P, P(CH₃)₃), 30.9 (dd, ²J_{P,P} = 48 Hz, 24 Hz, 1P, P(CH₃)₃), 28.5 (m, 1P, P(CH₃)₃). ¹³C NMR (75 MHz, C₆D₆, 298 K, ppm): 25.4 (d, ²J_{P,C} = 15 Hz, P(CH₃)₃), 26.8 (dd, ²J_{P,C} = 23 Hz, 8 Hz, P(CH₃)₃), 29.2 (d, ²J_{P,C} = 15 Hz, P(CH₃)₃), 31.6 (C(CH₃)₃), 32.1 (C(CH₃)₃), 32.7 (CH₃), 53.3 (C(CH₃)₃), 54.5 (C(CH₃)₃), 111.3 (C_{arom}), 129.4 (C_{arom}), 129.5 (C_{arom}), 132.2 (C_{arom}), 139.6 (C_{arom}), 150.9 (C_{arom}), 152.2 (C_{arom}), 152.4 (C_{arom}), 152.5 (C_{arom}), 172.0 (NCN). ²⁹Si NMR (99 MHz, C₆D₆, 298 K, ppm): 57.8 (ddd, ²J_{P,Si} = 89.1 Hz, 49.5 Hz, 19.8 Hz).

General Procedure for Iron-Catalyzed Hydroboration Reactions. Under a N₂ atmosphere, 1 mol % iron hydride complex **2** (4.32 mg, 5 μmol) in THF (1 mL) was added to a 20 mL Schlenk tube containing a magnetic stirrer. The ketone or aldehyde (1.0 mmol) and pinacolborane (140.8 mg, 1.1 mmol) were then weighed and added. The reaction mixture was allowed to stir at room temperature for the indicated time. After completion of the reaction, the solvent was evaporated, and the crude reaction mixture was purified by flash column chromatography with SiO₂ using a mixture of petroleum ether and ethyl acetate (5:1) as an eluent. The pure products were characterized by ¹H NMR analysis.

X-ray Crystal Structure Determinations. Single-crystal X-ray diffraction data for the complexes were collected on a XtaLAB AFC12 (RINC) (**1**) or Stoe Stadi Vari (**2**) diffractometer equipped with graphite-monochromatized Mo Kα radiation (λ = 0.71073 Å). During collection of the intensity data, no significant decay was observed. The intensities were corrected for Lorentz polarization effects and empirical absorption with the SADABS program. The structures were resolved by direct or Patterson methods with the OLEX2 program⁴⁴ and refined on F² with SHELXL.⁴⁵ All non-hydrogen atoms were refined anisotropically. Hydrogen atoms were included in calculated positions and were refined using a riding model.

Theoretical Calculations. DFT calculations on complex **2** were performed with the B3LYP functional using the LANL2DZ basis set for Fe and the 6-31G(d,p) basis set for the other atoms using the Gaussian 03 program package. Optimized structures of model compounds were obtained without symmetry constraints.

■ ASSOCIATED CONTENT

Supporting Information

The Supporting Information is available free of charge on the ACS Publications website at DOI: 10.1021/acs.organomet.8b00700.

Crystallographic data for **1** and **2**; IR and ¹H, ³¹P, ¹³C, and ²⁹Si NMR spectra of **1** and **2**; ¹H NMR spectra of the hydroboration reduction products; and IR, ¹H and ¹⁹F NMR, and MS spectra for the study of the catalytic mechanism; and computational details (PDF)

Accession Codes

CCDC 1537480 and 1587507 contain the supplementary crystallographic data for this paper. These data can be obtained free of charge via www.ccdc.cam.ac.uk/data_request/cif, or by e-mailing data_request@ccdc.cam.ac.uk, or by contacting The Cambridge Crystallographic Data Centre, 12 Union Road, Cambridge CB2 1EZ, U.K.; fax: +44 1223 336033.

AUTHOR INFORMATION

Corresponding Authors

*E-mail: xli63@sdu.edu.cn.

*E-mail: hjsun@sdu.edu.cn.

ORCID

Xia Zuo: 0000-0001-5205-5300

Xiaoyan Li: 0000-0003-0997-0380

Hongjian Sun: 0000-0003-1237-3771

Notes

The authors declare no competing financial interest.

ACKNOWLEDGMENTS

We thank the National Natural Science Foundation of China (21572119).

REFERENCES

- (1) (a) Asay, M.; Jones, C.; Driess, M. N-Heterocyclic Carbene Analogues with Low-Valent Group 13 and Group 14 Elements: Syntheses, Structures, and Reactivities of a New Generation of Multitalented Ligands. *Chem. Rev.* **2011**, *111*, 354–396. (b) Sen, S. S.; Khan, S.; Samuel, P. P.; Roesky, H. W. Chemistry of Functionalized Silylenes. *Chem. Sci.* **2012**, *3*, 659–682. (c) Blom, B.; Gallego, D.; Driess, M. N-Heterocyclic Silylene Complexes in Catalysis: New Frontiers in an Emerging Field. *Inorg. Chem. Front.* **2014**, *1*, 134–148. (d) Álvarez-Rodríguez, L.; Cabeza, J. A.; García-Álvarez, P.; Polo, D. The Transition-Metal Chemistry of Amidinosilylenes, -germylenes and -stannylenes. *Coord. Chem. Rev.* **2015**, *300*, 1–28. (e) Raouf-moghaddam, S.; Zhou, Y.-P.; Wang, Y.; Driess, M. N-Heterocyclic Silylenes as Powerful Steering Ligands in Catalysis. *J. Organomet. Chem.* **2017**, *829*, 2–10.
- (2) Furstner, A.; Krause, H.; Lehmann, C. W. Preparation, Structure and Catalytic Properties of a Binuclear Pd(0) Complex with Bridging Silylene Ligands. *Chem. Commun.* **2001**, 2372–2373.
- (3) Zhang, M.; Liu, X.; Shi, C.; Ren, C.; Ding, Y.; Roesky, H. W. The Synthesis of $(\eta^3\text{-C}_3\text{H}_5)_2\text{Pd}\{\text{Si}[\text{N}(\text{tBu})\text{CH}_2]_2\}\text{Cl}$ and the Catalytic Property for Heck Reaction. *Z. Anorg. Allg. Chem.* **2008**, *634*, 1755–1758.
- (4) Stoelzel, M.; Präsang, C.; Blom, B.; Driess, M. N-Heterocyclic Silylene (NHSi) Rhodium and Iridium Complexes: Synthesis, Structure, Reactivity, and Catalytic Ability. *Aust. J. Chem.* **2013**, *66*, 1163–1170.
- (5) (a) Brück, A.; Gallego, D.; Wang, W.; Irran, E.; Driess, M.; Hartwig, J. F. Pushing the s-Donor Strength in Iridium Pincer Complexes: Bis-(silylene) and Bis(germylene) Ligands Are Stronger Donors than Bis(phosphorus(III)) Ligands. *Angew. Chem., Int. Ed.* **2012**, *51*, 11478–11482. (b) Ren, H.; Zhou, Y.-P.; Bai, Y.; Cui, C.; Driess, M. Cobalt-Catalyzed Regioselective Borylation of Arenes: N-Heterocyclic Silylene as an Electron Donor in the Metal-Mediated Activation of C-H Bonds. *Chem. - Eur. J.* **2017**, *23*, 5663–5667.
- (6) Zhou, Y.-P.; Raouf-moghaddam, S.; Szilvási, T.; Driess, M. A Bis(silylene)-Substituted ortho-Carborane as a Superior Ligand in the Nickel-Catalyzed Amination of Arenes. *Angew. Chem., Int. Ed.* **2016**, *55*, 12868–12878.
- (7) Wang, W.; Inoue, S.; Enthaler, S.; Driess, M. Bis(silylenyl)- and Bis(germylenyl)-Substituted Ferrocenes: Synthesis, Structure, and Catalytic Applications of Bidentate Silicon(II)–Cobalt Complexes. *Angew. Chem., Int. Ed.* **2012**, *51*, 6167–6171.
- (8) (a) Iimura, T.; Akasaka, N.; Iwamoto, T. A Dialkylsilylene-Pt(0) Complex with a DVTMS Ligand for the Catalytic Hydrosilylation of Functional Olefins. *Organometallics* **2016**, *35*, 4071–4076. (b) Iimura, T.; Akasaka, N.; Kosai, T.; Iwamoto, T. A Pt(0) Complex with Cyclic (alkyl)(amino)silylene and 1,3-Divinyl-1,1,3,3-tetramethyldisiloxane Ligands: Synthesis, Molecular Structure, and Catalytic Hydrosilylation Activity. *Dalton Trans.* **2017**, *46*, 8868–8874.
- (9) (a) Blom, B.; Enthaler, S.; Inoue, S.; Irran, E.; Driess, M. Electron-Rich N-Heterocyclic Silylene (NHSi)–Iron Complexes: Synthesis, Structures, and Catalytic Ability of an Isolable Hydridosilylene–Iron Complex. *J. Am. Chem. Soc.* **2013**, *135*, 6703–6713. (b) Gallego, D.; Inoue, S.; Blom, B.; Driess, M. Highly Electron-Rich Pincer-Type Iron Complexes Bearing Innocent Bis(metallylene)pyridine Ligands: Syntheses, Structures, and Catalytic Activity. *Organometallics* **2014**, *33*, 6885–6897.
- (10) Gallego, D.; Brück, A.; Irran, E.; Meier, F.; Kaupp, M.; Driess, M.; Hartwig, J. F. From Bis(silylene) and Bis(germylene) Pincer-Type Nickel(II) Complexes to Isolable Intermediates of the Nickel-Catalyzed Sonogashira Cross-Coupling Reaction. *J. Am. Chem. Soc.* **2013**, *135*, 15617–15626.
- (11) (a) Someya, C. I.; Haberberger, M.; Wang, W.; Enthaler, S.; Inoue, S. Application of a Bis(silylene) Nickel Complex as Precatalyst in C–C Bond Formation Reactions. *Chem. Lett.* **2013**, *42*, 286–288. (b) Tan, G.; Enthaler, S.; Inoue, S.; Blom, B.; Driess, M. Synthesis of Mixed Silylene–Carbene Chelate Ligands from N-Heterocyclic Silylcarbenes Mediated by Nickel. *Angew. Chem.* **2015**, *127*, 2242–2246.
- (12) (a) Cho, B. T. Recent Development and Improvement for Boron Hydride-based Catalytic Asymmetric Reduction of Unsymmetrical Ketones. *Chem. Soc. Rev.* **2009**, *38*, 443–452. (b) Magano, J.; Dunetz, J. R. Large-Scale Carbonyl Reductions in the Pharmaceutical Industry. *Org. Process Res. Dev.* **2012**, *16*, 1156–1184. (c) Miyaura, N. Hydroboration, Diboration, Silylboration, and Stannylboration. In *Catalytic Heterofunctionalization*; Togni, A., Grützmacher, H., Eds.; Wiley-VCH: Weinheim, Germany, 2001; pp 1–45. (d) Chong, C. C.; Kinjo, R. Catalytic Hydroboration of Carbonyl Derivatives, Imines, and Carbon Dioxide. *ACS Catal.* **2015**, *5*, 3238–3259.
- (13) Kaithal, A.; Chatterjee, B.; Gunanathan, C. Ruthenium Catalyzed Selective Hydroboration of Carbonyl Compounds. *Org. Lett.* **2015**, *17*, 4790–4793.
- (14) Bagherzadeh, S.; Mankad, N. P. Extremely Efficient Hydroboration of Ketones and Aldehydes by Copper Carbene Catalysis. *Chem. Commun.* **2016**, *52*, 3844–3846.
- (15) (a) Giffels, G.; Dreisbach, C.; Kragl, U.; Weigerding, M.; Waldmann, H.; Wandrey, C. Chiral Titanium Alkoxides as Catalysts for the Enantioselective Reduction of Ketones with Boranes. *Angew. Chem., Int. Ed. Engl.* **1995**, *34*, 2005–2006. (b) Almqvist, F.; Torstensson, L.; Gudmundsson, A.; Frejd, T. New Ligands for the Titanium(rv)-Induced Asymmetric Reduction of Ketones with Catecholborane. *Angew. Chem., Int. Ed. Engl.* **1997**, *36*, 376–377. (c) Sarvary, I.; Almqvist, F.; Frejd, T. Asymmetric Reduction of Ketones with Catecholborane Using 2,6-BODOL Complexes of Titanium(IV) as Catalysts. *Chem. - Eur. J.* **2001**, *7*, 2158–2166. (d) Oluyadi, A. A.; Ma, S.; Muhoro, C. N. Titanocene(II)-Catalyzed Hydroboration of Carbonyl Compounds. *Organometallics* **2013**, *32*, 70–78.
- (16) Khalimon, A. Y.; Farha, P.; Kuzmina, L. G.; Nikonov, G. I. Catalytic Hydroboration by an Imido-Hydrido Complex of Mo(IV). *Chem. Commun.* **2012**, *48*, 455–457.
- (17) Zhang, G.; Zeng, H.; Wu, J.; Yin, Z.; Zheng, S.; Fettinger, J. C. Highly Selective Hydroboration of Alkenes, Ketones and Aldehydes Catalyzed by a Well-Defined Manganese Complex. *Angew. Chem.* **2016**, *128*, 14581–14584.
- (18) (a) Roh, S.-G.; Park, Y.-C.; Park, D.-K.; Kim, T.-J.; Jeong, J. H. Synthesis and Characterization of a Zn(II) Complex of a Pyrazole-Based Ligand Bearing a Chiral L-Alaninemethylester. *Polyhedron* **2001**, *20*, 1961–1965. (b) Locatelli, M.; Cozzi, P. G. Effective Modular Iminooxazoline (IMOX) Ligands for Asymmetric Catalysis: [Zn-(IMOX)]-Promoted Enantioselective Reduction of Ketones by Catecholborane. *Angew. Chem.* **2003**, *115*, 5078–5080. (c) Roh, S.

- G.; Yoon, J. U.; Jeong, J. H. Synthesis and Characterization of a Chiral Zn(II) Complex Based on a trans-1,2-Diaminocyclohexane Derivative and Catalytic Reduction of Acetophenone. *Polyhedron* **2004**, *23*, 2063–2067. (d) Lummis, P. A.; Momeni, M. R.; Lui, M. W.; McDonald, R.; Ferguson, M. J.; Miskolzie, M.; Brown, A.; Rivard, E. Accessing Zinc Monohydride Cations through Coordinative Interactions. *Angew. Chem., Int. Ed.* **2014**, *53*, 9347–9351.
- (19) (a) Mukherjee, D.; Osseili, H.; Spaniol, T. P.; Okuda, J. Alkali Metal Hydridotriphenylborates [(L)M][HBPh₃] (M = Li, Na, K): Chemoselective Catalysts for Carbonyl and CO₂ Hydroboration. *J. Am. Chem. Soc.* **2016**, *138*, 10790–10793. (b) Zhu, Z.; Wu, X.; Xu, X.; Wu, Z.; Xue, M.; Yao, Y.; Shen, Q.; Bao, X. n-Butyllithium Catalyzed Selective Hydroboration of Aldehydes and Ketones. *J. Org. Chem.* **2018**, *83*, 10677–10683.
- (20) (a) Arrowsmith, M.; Hadlington, T. J.; Hill, M. S.; Kociok-Köhn, G. Magnesium-Catalyzed Hydroboration of Aldehydes and Ketones. *Chem. Commun.* **2012**, *48*, 4567–4569. (b) Manna, K.; Ji, P.; Greene, F. X.; Lin, W. Metal–Organic Framework Nodes Support Single-Site Magnesium–Alkyl Catalysts for Hydroboration and Hydroamination Reactions. *J. Am. Chem. Soc.* **2016**, *138*, 7488–7491. (c) Lampland, N. L.; Hovey, M.; Mukherjee, D.; Sadow, A. D. Magnesium-Catalyzed Mild Reduction of Tertiary and Secondary Amides to Amines. *ACS Catal.* **2015**, *5*, 4219–4226.
- (21) Yadav, S.; Pahar, S.; Sen, S. S. Benz-Amidinato Calcium Iodide Catalyzed Aldehyde and Ketone Hydroboration with Unprecedented Functional Group Tolerance. *Chem. Commun.* **2017**, *53*, 4562–4564.
- (22) (a) Yang, Z.; Zhong, M.; Ma, X.; Nijesh, K.; De, S.; Parameswaran, P.; Roesky, H. W. An Aluminum Dihydride Working as a Catalyst in Hydroboration and Dehydrocoupling. *J. Am. Chem. Soc.* **2016**, *138*, 2548–2551. (b) Jakhar, V. K.; Barman, M. K.; Nembenna, S. Aluminum Monohydride Catalyzed Selective Hydroboration of Carbonyl Compounds. *Org. Lett.* **2016**, *18*, 4710–4713.
- (23) Blake, A. J.; Cunningham, A.; Ford, A.; Teat, S. J.; Woodward, S. Enantioselective Reduction of Prochiral Ketones by Catecholborane Catalyzed by Chiral Group 13 Complexes. *Chem. - Eur. J.* **2000**, *6*, 3586–3594.
- (24) Hadlington, T. J.; Hermann, M.; Frenking, G.; Jones, C. Low Coordinate Germanium(II) and Tin(II) Hydride Complexes: Efficient Catalysts for the Hydroboration of Carbonyl Compounds. *J. Am. Chem. Soc.* **2014**, *136*, 3028–3031.
- (25) Chong, C. C.; Hirao, H.; Kinjo, R. Metal-Free s-Bond Metathesis in 1,3,2-Diazaphospholene-Catalyzed Hydroboration of Carbonyl Compounds. *Angew. Chem., Int. Ed.* **2015**, *54*, 190–194.
- (26) (a) Weidner, V. L.; Barger, C. J.; Delferro, M.; Lohr, T. L.; Marks, T. J. Rapid, Mild, and Selective Ketone and Aldehyde Hydroboration Reduction Mediated by a Simple Lanthanide Catalyst. *ACS Catal.* **2017**, *7*, 1244–1247. (b) Chen, S.; Yan, D.; Xue, M.; Hong, Y.; Yao, Y.; Shen, Q. Tris(cyclopentadienyl)lanthanide Complexes as Catalysts for Hydroboration Reaction toward Aldehydes and Ketones. *Org. Lett.* **2017**, *19*, 3382–3385. (c) Yan, D.; Dai, P.; Chen, S.; Xue, M.; Yao, Y.; Shen, Q.; Bao, X. Highly Efficient Hydroboration of Carbonyl Compounds Catalyzed by Tris (Methylcyclopentadienyl)lanthanide Complexes. *Org. Biomol. Chem.* **2018**, *16*, 2787–2791. (d) Zhu, Z.; Dai, P.; Wu, Z.; Xue, M.; Yao, Y.; Shen, Q.; Bao, X. Lanthanide Aryloxides Catalyzed Hydroboration of Aldehydes and Ketones. *Catal. Commun.* **2018**, *112*, 26–30.
- (27) Guo, J.; Chen, J.; Lu, Z. Cobalt-Catalyzed Asymmetric Hydroboration of Aryl Ketones with Pinacolborane. *Chem. Commun.* **2015**, *51*, 5725–5727.
- (28) Tamang, S. R.; Findlater, M. Iron Catalyzed Hydroboration of Aldehydes and Ketones. *J. Org. Chem.* **2017**, *82*, 12857–12862.
- (29) Das, U. K.; Higman, C. S.; Gabidullin, B.; Hein, J. E.; Baker, R. T. Efficient and Selective Iron-Complex-Catalyzed Hydroboration of Aldehydes. *ACS Catal.* **2018**, *8*, 1076–1081.
- (30) Qi, X.; Sun, H.; Li, X.; Fuhr, O.; Fenske, D. Synthesis and Catalytic Activity of N-Heterocyclic Silylene (NHSi) Cobalt Hydride for Kumada Coupling Reactions. *Dalton Trans.* **2018**, *47*, 2581–2588.
- (31) So, C.-W.; Roesky, H. W.; Magull, J.; Oswald, R. B. Synthesis and Characterization of [PhC(NtBu)₂Si]Cl: A Stable Monomeric Chlorosilylene. *Angew. Chem., Int. Ed.* **2006**, *45*, 3948–3950.
- (32) Bhattacharya, P.; Krause, J. A.; Guan, H. Iron Hydride Complexes Bearing Phosphinite-Based Pincer Ligands: Synthesis, Reactivity, and Catalytic Application in Hydrosilylation Reactions. *Organometallics* **2011**, *30*, 4720–4729.
- (33) Schmedake, T. A.; Haaf, M.; Paradise, B. J.; Millevolte, A. J.; Powell, D. R.; West, R. Electronic and Steric Properties of Stable Silylene Ligands in Metal(0) Carbonyl Complexes. *J. Organomet. Chem.* **2001**, *636*, 17–25.
- (34) Yang, W.; Fu, H.; Wang, H.; Chen, M.; Ding, Y.; Roesky, H. W.; Jana, A. A Base-Stabilized Silylene with a Tricoordinate Silicon Atom as a Ligand for a Metal Complex. *Inorg. Chem.* **2009**, *48*, 5058–5060.
- (35) Eisenhut, C.; Szilvási, T.; Dübek, G.; Breit, N. C.; Inoue, S. Systematic Study of N-Heterocyclic Carbene Coordinate Hydro-silylene Transition-Metal Complexes. *Inorg. Chem.* **2017**, *56*, 10061–10069.
- (36) Tobita, H.; Matsuda, A.; Hashimoto, H.; Ueno, K.; Ogino, H. Direct Evidence for Extremely Facile 1,2- and 1,3-Group Migrations in an FeSi₂ System. *Angew. Chem., Int. Ed.* **2004**, *43*, 221–224.
- (37) Basis sets employed: B3LYP/6-31G(d,p) for C, H, N, P, and Si; LANL2DZ for Fe. The calculations were performed using Gaussian 03, revision D.01.
- (38) (a) Wiberg, K. B. Application of the Pople-Santry-Segal CNDO Method to the Cyclopropylcarbinyl and Cyclobutyl Cation and to Bicyclobutane. *Tetrahedron* **1968**, *24*, 1083–1096. (b) Irwin, R. P. *Organometallic Chemistry: Research Perspectives*, 1st ed.; Nova Science Publishing: Hauppauge, NY, 2008; p 292.
- (39) (a) Schneck, F.; Assmann, M.; Balmer, M.; Harms, K.; Langer, R. Selective Hydrogenation of Amides to Amines and Alcohols Catalyzed by Improved Iron Pincer Complexes. *Organometallics* **2016**, *35*, 1931–1943. (b) Jayarathne, U.; Zhang, Y.; Hazari, N.; Bernskoetter, W. H. Selective Iron-Catalyzed Deaminative Hydrogenation of Amides. *Organometallics* **2017**, *36*, 409–416.
- (40) (a) Li, H.; Misal Castro, L. C.; Zheng, J.; Roisnel, T.; Dorcet, V.; Sortais, J.-B.; Darcel, C. Selective Reduction of Esters to Aldehydes under the Catalysis of Well-Defined NHC–Iron Complexes. *Angew. Chem.* **2013**, *125*, 8203–8207. (b) Blom, B.; Tan, G.; Enthaler, S.; Inoue, S.; Epping, J. D.; Driess, M. Bis-N-Heterocyclic Carbene (NHC) Stabilized η⁶-Arene Iron(0) Complexes: Synthesis, Structure, Reactivity, and Catalytic Activity. *J. Am. Chem. Soc.* **2013**, *135*, 18108–18120.
- (41) Karsch, H. H. Funktionelle Trimethylphosphinderivate, V. Kovalente Methyleisen (II)-Phosphinkomplexe. *Chem. Ber.* **1977**, *110*, 2699–2711.
- (42) Sen, S. S.; Roesky, H. W.; Stern, D.; Henn, J.; Stalke, D. High Yield Access to Silylene RSiCl (R = PhC(NtBu)₂) and Its Reactivity toward Alkyne: Synthesis of Stable Disilacyclobutene. *J. Am. Chem. Soc.* **2010**, *132*, 1123–1126.
- (43) Smart, K. A.; Grellier, M.; Vendier, L.; Mason, S. A.; Capelli, S. C.; Albinati, A.; Sabo-Etienne, S. Step-by-Step Introduction of Silazane Moieties at Ruthenium: Different Extents of Ru–H–Si Bond Activation. *Inorg. Chem.* **2013**, *52*, 2654–2661.
- (44) Dolomanov, O. V.; Bourhis, L. J.; Gildea, R. J.; Howard, J. A. K.; Puschmann, H. OLEX2: a Complete Structure Solution, Refinement and Analysis Program. *J. Appl. Crystallogr.* **2009**, *42*, 339–341.
- (45) Sheldrick, G. M. SHELXT - Integrated Space-Group and Crystal-Structure Determination. *Acta Crystallogr., Sect. A: Found. Adv.* **2015**, *71*, 3–8.